Laser-induced Luminescence Technique for the Simultaneous Measurement of Local Film Thickness and Temperature Distribution in Thin Wavy Liquid Films

A. Schagen and M. Modigell
Department of Chemical Engineering
RWTH Aachen University
Turmstr. 46, D - 52064 Aachen,
Germany
schagen@ivt.rwth-aachen.de and modigell@ivt.rwth-aachen.de at http://www.ivt.rwth-aachen.de

Abstract: Heat transfer in falling liquid film systems is enhanced by waviness. Comprehension of the underlying kinetic phenomena requires experimental data of the temperature field with high spatiotemporal resolution. Therefore a non-invasive measuring method based on luminescence indicators is developed. It is used to determine the temperature distribution and the local film thickness simultaneously. Results are presented for the temperature distribution measurement in a laminar-wavy water film with a liquid side Reynolds number of 126 flowing down a heated plane with an inclination angle of 2°. The measured temperature distributions are used to calculate the local heat transfer coefficient for solitary waves at two positions in flow direction.

Key-Words: falling film, wave induced enhancement of heat transfer, local heat transfer coefficient

Nomenclature

C	molar concentration, mol/m^3
d	thickness, diameter, m
f	frequency, 1/s
H	height of channel, m
I	intensity, W/m^2
K	constant device factor, V m/W
L	length of channel, m
M	measured signal, V
n	distribution of effective emission area, m^2
N	number of nodal points
Pr	Prandtl number $= \nu/\kappa$
Re	Reynolds number $= \dot{V}/(\nu\, W)$
t	time, s
u	streamwise velocity, m/s
v	transversal velocity, m/s
V	volume, m^3
W	width of channel, m
x	streamwise coordinate, m
y	normal coordinate, m

greek symbols

α	heat transfer coefficient, W/(m^2 K)
η	dynamic viscosity, kg/(m s)
φ	inclination angle, $^\circ$
κ	thermal diffusivity, m^2/s
λ	thermal conductivity, W/(m K)
λ	wave length, m
ν	kinematic viscosity, m^2/s
ϑ	temperature, °C
ρ	density, kg/m^3
τ	decay constant, s

subscripts

d	disturbance
exp	experimental
f	film
g	gas
i	interface
l	liquid, lower bound
m	mean
Nu	Nusselt
ob	observation volume
P	phosphorescence
sta	stagnant liquid
u	upper bound
w	wave, wall

superscripts

*	scaled value

1 Introduction

The liquid phase in applications of chemical and life science industry, like film evaporators, absorption heat pumps and falling film reactors, often occurs as gravity driven flow in form of thin liquid films. It is observed that heat and mass transfer in wavy film flow is significantly higher than in a smooth film. A variety of investigations have been performed to analyze heat and mass transfer resulting in

semi-empirical correlations to describe transfer enhancement in such film systems, see Brauner and Maron (1982) [9], Wasden and Dukler (1990) [24], Conslisk (1995) [11], Alhusseini et al. (1998) [2], Roberts and Chang (2000) [20] and Miladinova et al. (2002) [17]. For a critical review of models of coupled heat and mass transfer in falling film absorption see Killion and Garimella (2001) [14]. The mechanisms of transport processes leading to the enhancement of heat transfer in such systems are not clarified in detail. Because of the complexity of the system it is not possible to identify the responsible transport mechanism from integral measurements of heat transport.

To analyze these phenomena in detail, heat transfer in falling liquid films is investigated in the Collaborative Research Center (SFB) 540 "Model-based Experimental Analysis of Kinetic Phenomena in Multi-phase Fluid Reactive Systems". To gain deeper insight two essential objectives were pursued: to identify the precise hydrodynamic regime in falling liquid films and to obtain highly resolved experimental data on the temperature distribution in a heated film.

The small film thickness requires a non invasive measuring method to avoid disturbance of the film. There exist some well developed non-invasive optical measurement techniques e.g. laser doppler anemometry (LDA) and particle image velocimetry (PIV) for velocity field measurement. Measurements of the velocity field in wavy film flow were performed by Al-Sibai et al. (2002) [6]. For information about local film thickness a chromatic confocal imaging method can be used, see Lel et al. (2004) [15]. For temperature field measurements thermo-chromic liquid crystals (TLC) were used. For example Günther and Rudolf von Rohr (2002) [21] measured temperature and velocity fields in turbulent natural convection by combining PIV and liquid crystal thermography (LCT). In order to get field information about velocity and temperature simultaneously a combination of PIV and planar laser induced fluorescence (PLIF) is used. Hishida and Sakakibara (2000) [13] used this method to investigate impinging jets. In the cases where PLIF is used to get information about the temperature distribution, the region of interest has to be optically accessible in two perpendicular planes to realize the planar laser sheet and to measure the emission of the excited indicator. This results in certain geometrical restrictions for the systems to be investigated.

The proposed optical method presented in this paper makes use of optical probes which allow to provide the temperature distribution in a film flowing down a heated plane and the local film thickness simultaneously in both high spatial and high temporal resolution. The measurements are possible at several user-defined points of interest at the same time. The data obtained from the presented measurements is used to determine the local heat transfer coefficients in single waves.

2 Physical Basics

For the investigation of the heat transport in a laminar wavy liquid film of water the optical indicator biacetyl (2,3-butanedione) is used. Biacetyl has a molar mass of 86.09 g/mol and a density of 0.99 g/cm^3 (20 °C). It emits phosphorescence as well as fluorescence when illuminated with UV-light. In an aqueous solution the phosphorescence and fluorescence intensity depend on temperature and indicator concentration. Furthermore the phosphorescence is quenched by dissolved oxygen in the water whereas the intensity of fluorescence is independent of oxygen. The latter interrelationship was used to measure concentration distributions C of absorbed oxygen in laminar wavy liquid films, see Schagen and Modigell (2005) [23].

After a pulsed excitation with UV-light the phosphorescence emission I decreases with time according to

$$I(C,\vartheta,t) \;=\; I_0(C,\vartheta)\, e^{-t/\tau(C,\vartheta)} \quad . \tag{1}$$

In this equation I_0 is the initial emission intensity after turning off the excitation and τ is the decay constant of the phosphorescence emission.

In this work only oxygen free aqueous solution ($C = 0$) is used and so the phosphorescence emission depends only on temperature. Measurements have been performed to analyze the correlation between the temperature and the decay constant of the phosphorescence emission using the optical device described in Sect. 4.1. A tempered glass vessel, equipped with a thermocouple and a magnetic stirrer, was filled with 1 l of demineralized water, which was stripped of dissolved oxygen with purified nitrogen bubbles. After the degasification the luminescence indicator biacetyl was added in a concentration of 11.4 mol/m^3. This biacetyl concentration was used by Bäckström and Sandros (1958) [10] in their experiments to determine the decay constant of the phosphorescence emission. The concentration of biacetyl is very low compared to the solubility concentration of 285 mol/m^3 to prevent self quenching of the emission. The temperature dependency of the phosphorescence decay constant was measured in the range from 10 to 30 °C as depicted in Fig. 1.

The experimental data can be approximated with the linear equation

$$\tau(\vartheta) \;=\; -3.4\times10^{-6}\mathrm{s/^\circ C}\cdot\vartheta \;+\; 2.99\times10^{-4}\mathrm{s} \tag{2}$$

with a residual norm of 2.94×10^{-6} and a mean standard deviation of 2.3×10^{-5} s. The measurement at ϑ = 20 °C is in good agreement with the value of Bäckström and Sandros (1958) [10] who reported a value of $\tau = 229$ μs. The measurement of Almgren (1967) [4] of 201 μs at 25 °C was obtained with a higher concentration of biacetyl in aqueous solution which possibly caused self quenching of the phosphorescence emission.

By measuring the decay of the phosphorescence in an isothermal system of aqueous biacetyl solution the temperature can be simply determined. Describing the measured

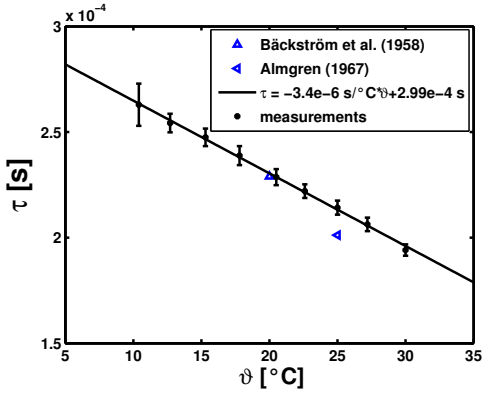

Figure 1: Decay constant of biacetyl phosphorescence in an oxygen free aqueous solution depending on temperature.

data by applying Eq. (1) the decay constant τ is obtained. Finally, making use of Eq. (2), the temperature can be calculated.

In case of a non-uniform temperature distribution in a stagnant liquid film every volume element emits a specific phosphorescence after excitation, depending on the local temperature, as sketched in Fig. 2.

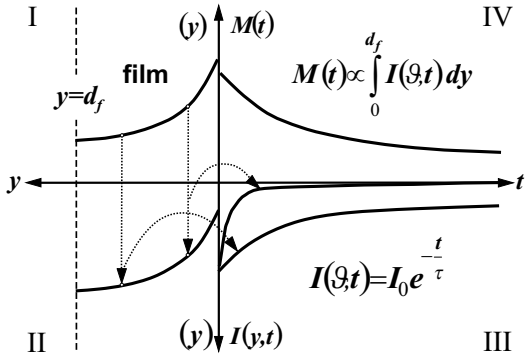

Figure 2: Dependence of measured signal $M(t)$ on temperature profile $\vartheta(y)$ in a stagnant liquid film.

In quadrant I a temperature profile in a liquid film is qualitatively shown as a function of the coordinate y, which is oriented perpendicular to the surface of the film. The surface of the film is indicated by d_f. Quadrant II shows the corresponding course of the local decay constant also as a function of y. The local initial intensity and the respective time dependent specific phosphorescence intensity emitted from two locations in the film, indicated with the arrows, are drawn in quadrant III. The phosphorescence totally emitted by all volume elements along the coordinate y is given by the integral equation

$$M_{\mathrm{P,sta}}(t) = K \int_0^{d_\mathrm{f}} I(\vartheta, t)\, dy \qquad (3)$$

as indicated in quadrant IV in Fig. 2. The factor K in Eq. (3) contains apparatus and device specific contributions to the optical signal which can be assumed to be constant.

Finally, the total intensity M emitted by the observation volume in a flowing liquid film is influenced by the velocity distribution $u(y)$. During the measurement volume elements containing excited biacetyl molecules move out of the fixed observation volume due to their local velocities. The resulting superposed decrease of the measured signal can be modelled based on the residence time of excited biacetyl molecules within the observation volume. This leads to

$$M_\mathrm{P}(t) = K \int_0^{d_\mathrm{f}} n_\mathrm{I}(y,t)\, I(\vartheta, t)\, dy \quad , \qquad (4)$$

where n_I is the distribution of the luminescent area within the cross section of the measurement volume, see Fig. 3, and can be modelled as

$$n_\mathrm{I}(y,t) = \frac{2}{\pi}\left[\arccos\left(\frac{u(y)\,t}{d_\mathrm{ob}}\right) - \frac{u(y)\,t}{d_\mathrm{ob}^2}\left(d_{ob}^2 - (u(y)\,t)^2\right)^{1/2}\right] \qquad (5)$$

using basic geometrical relations.

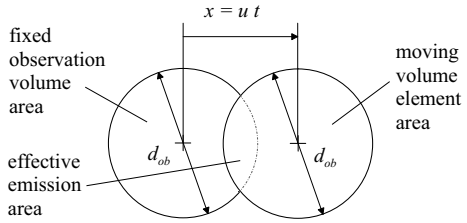

Figure 3: Effective emission area of a volume element within the moving liquid film.

The exact velocity field in our experiment is unknown. Yet the velocity distribution in flow direction $u(y)$ in wavy films can be approximated by a parabolic profile

$$u(y) = u_\mathrm{max}\left[2\frac{y}{d_\mathrm{f}} - \left(\frac{y}{d_\mathrm{f}}\right)^2\right] \qquad (6)$$

comparable to the analytical solution of Nusselt (1916) [18]. Here the parameter u_max is the longitudinal component of the local surface velocity, see e.g. Alekseenko et al. (1994) [3] and Al-Sibai et al. (2002) [6]. Based on experimental investigations on film flow of Adomeit et al. (2000) [1] and Al-Sibai et al. (2002) [6] we propose a linear interpolation of the surface velocity within the film thickness region $d_\mathrm{f,m} < d_\mathrm{f} < d_\mathrm{max}$. Thus the longitudinal surface velocity component can be calculated:

for $d_\mathrm{f} \le d_\mathrm{f,m}$: $u_\mathrm{max} = u_\mathrm{max,Nu} = \frac{g\,\sin\varphi}{\nu} d_\mathrm{f}^2$
for $d_\mathrm{f,m} < d_\mathrm{f} < d_\mathrm{f,max}$:
$u_\mathrm{max} = u_\mathrm{max,Nu} + (u_\mathrm{w} - u_\mathrm{max,Nu})\frac{d_\mathrm{f} - d_\mathrm{f,m}}{d_\mathrm{f,max} - d_\mathrm{f,m}}$
for $d_\mathrm{f} = d_\mathrm{f,max}$: $u_\mathrm{max} = u_\mathrm{w}$

The stream wise velocity u_w at the interface in the wave peak and the local instantaneous film thickness d_f are determined using the LIF technique. Thereby u_w is approximated with the wave peak velocity c_w which in turn is determined from a two point measurement using a cross correlation method reported for example in Al-Sibai (2005) [5].

The temperature dependency of the fluorescence shows only a small influence on the signal height of the fluorescence emission. Increasing the temperature results in a slight decrease of the signal. Comparable behavior is shown by the fluorescence indicator Rhodamine 110 which is used by Sakakibara and Adrian (1999) [22]. At constant biacetyl concentration the fluorescence emission solely depends on the film thickness. With appropriate calibration of the measuring device this allows for an accurate measurement of the film thickness.

Before carrying out the experiments some preliminary model-based investigations were done to examine the influence of the distribution of the local relaxation constant, the temperature distribution respectively, and the velocity distribution on the phosphorescence signal decay.

The analytical derivatives of the signal model with respect to these input parameters are:

$$\frac{\partial M_\mathrm{P}}{\partial \tau} = K \int_0^\delta n_\mathrm{I}(y,t)\, \frac{t}{\tau^2}\, e^{-t/\tau(y)}\, dy \qquad (7)$$

and

$$\frac{\partial M_\mathrm{P}}{\partial u} = -K \int_0^\delta \frac{2}{\pi} \left[2\, \frac{t}{d_\mathrm{ob}^2} g(y,t) \right] e^{-t/\tau(y)}\, dy \qquad (8)$$

with

$$g(y,t) = \sqrt{d_\mathrm{ob}^2 - (u(y)\, t)^2} \qquad (9)$$

Sensitivity calculations were performed using the temperature distribution in Fig. 4 with the resulting distribution of the local relaxation constants. The local film thickness is assumed to be d_f = 1 mm and for the velocity distribution a parabolic Nusselt profile with u_max = 0.5 m/s is used. The diameter of the observation volume is d_ob = 1 mm.

The resulting courses of the derivatives of the normalized phosphorescence M_P decay curves are shown in Fig. 5 and 6. The derivatives are scaled with the local values of τ and u. The sensitivity of the signal with respect to the local relaxation constants is one order of magnitude higher compared to the influence of velocity distribution on the signal. Therefore using an approximative velocity distribution in the evaluation procedure is sufficient as long as the residence time of excited biacetyl molecules within the observation volume is large compared to the measuring time.

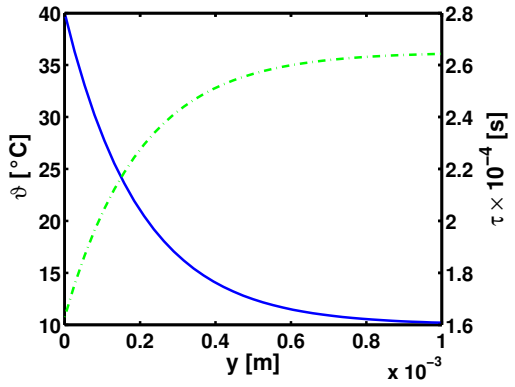

Figure 4: Assumed temperature and relaxation constant profiles for sensitivity investigation.

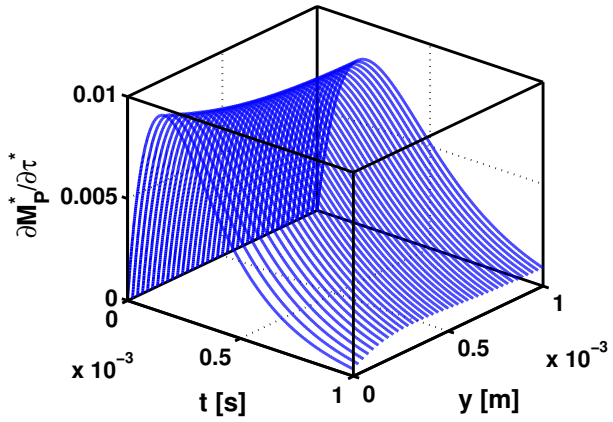

Figure 5: Sensitivity of phosphorescence signal with respect to the distribution of local relaxation constants from Fig. 4.

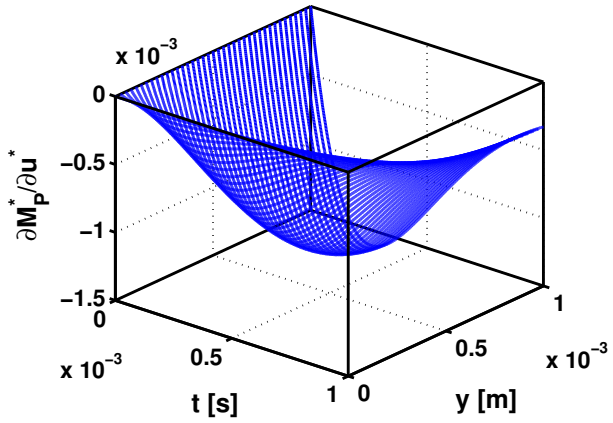

Figure 6: Sensitivity of phosphorescence signal with respect to the velocity distribution calculated using Eq. 6.

3 Evaluation Method

The objective of the evaluation method is to reconstruct the distribution of the local relaxation constant and temperature distribution $\vartheta(y)$ respectively from the measured time dependent optical signal $M(t)$ given by Eq. (4). Such a signal reconstruction is a classical inverse problem, see

e.g. Wolfersdorf (1994) [25], which in addition is nonlinear and ill-posed. One possibility to solve such a problem is to formulate an optimization task

$$\min_{\tau\in\mathbb{R}^N} F(\tau) = \min\left\{\frac{1}{2}\|M^*_{\mathrm{P,exp}} - M^*_{\mathrm{P}}\|_2^2 + \phi\|\frac{\partial^2\tau}{\partial y^2}\|_2^2\right\} \tag{10}$$

$$\text{s.t.} \quad \tau_{\mathrm{l}} \le \tau \le \tau_{\mathrm{u}} \quad ,$$

where $M^*_{\mathrm{P,exp}}$ represents the experimental data and M^*_{P} results from a model-based signal calculation using Eq. 4. The second term in the left hand side of the least square formulation is a regularization term which forces the estimate to be smooth. The regularization parameter ϕ is chosen to be 10^9 resulting from numerical investigations of the noised phosphorescence signals. This value balances the first and the second term of the least square formulation. The constraint condition restricts the solution τ to be within lower and upper bounds. The dimension N is chosen to be 39 for the numerical treatment of the defined optimization task. This is a compromise between computational cost and dependency of the signal on grid resolution in the y-coordinate. The numerical procedure makes use of a Trust-Region reflective Newton algorithm to which the analytical derivative of the signal with respect to τ, Eq. 7, is supplied.

The capability of the evaluation method to reconstruct the temperature distribution even from a noised phosphorescence decay signal was tested. A noised phosphorescence signal, see Fig. 7 is generated with a relaxation constant distribution converted from the temperature distribution "goal" in Fig. 8. The estimated relaxation constant distribution is converted back to the estimated temperature distribution. This reconstructed temperature profile fits the given temperature profile "goal" with reasonable accuracy.

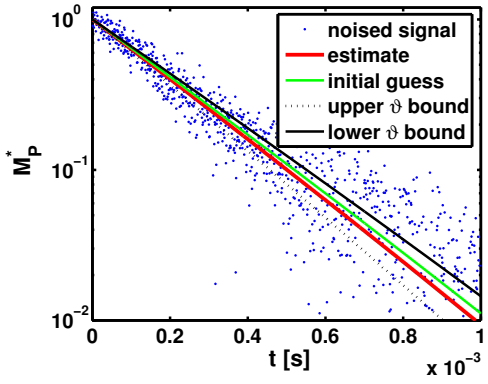

Figure 7: Signals calculated with the temperature distributions "goal","initial guess", "lower" and "upper bound", see Fig. 8, and reconstructed signal calculated with the "estimate".

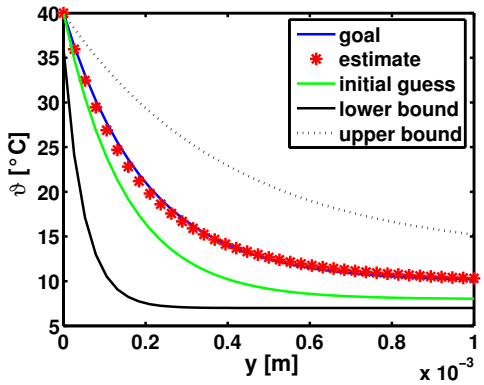

Figure 8: Reconstruction of the given temperature distribution "goal" by an "estimate" starting from an "initial guess".

4 Experimental Design

4.1 Optical Measuring Technique

The measuring device is basically a phosphoroscope. The source of the primary UV laser beam at a peak wave length of 405 nm is a nitrogen pumped dye laser with a maximum pulse frequency of 50 Hz. As laser dye 4,4'-diphenylstilbene (Lambda Physik AG, Germany) is used. The nitrogen laser pulse has an energy of 116 μJ at a pulse width of 700 ps. A beam splitter optic splits the primary beam into two beams that are sent through light conductors to excite probe volumes in the wavy film with a diameter of about 1 mm. The scheme of the measurement design is shown in Fig. 9.

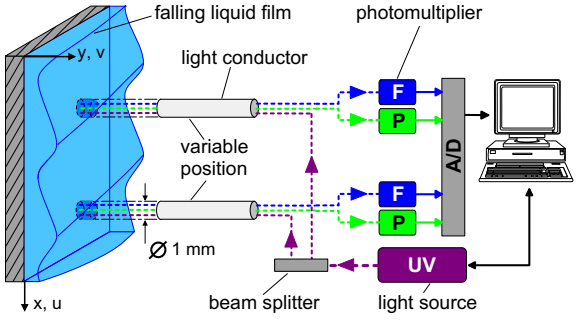

Figure 9: Principle of simultaneous two point measurement.

To obtain information on the wave peak velocity u_{w} which is needed to characterize the wave properties, the measurement has to be performed at two points in film flow direction simultaneously. The emission of the dissolved and homogeneously distributed biacetyl is measured with four photo-multipliers (Hamamatsu Photonics K.K., Japan). Two of the photo-multipliers measure the phosphorescence to get the temperature profile in the liquid film and the other two measure the fluorescence to get the local film thickness. To separate the information contain-

ing indicator emission from the (reflected) excitation light they are equipped with optical edge filters (Schott AG, Germany). For the separation of the phosphorescence edge filters GG 475 and for the separation of fluorescence OG 515 are used. Figure 10 shows the normalized spectra of excitation and luminescence emission of biacetyl measured with a LIMES-spectrometer (LTB GmbH, Germany).

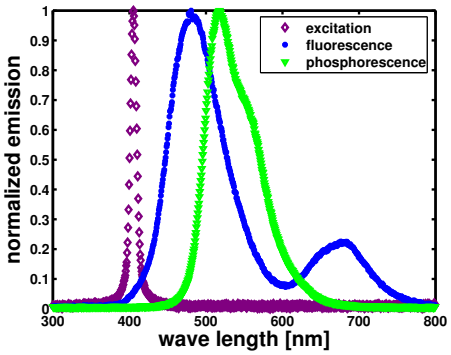

Figure 10: Normalized emission spectra of excitation, phosphorescence and fluorescence.

A spectral separation of fluorescence and phosphorescence is not possible. Here the separation is based on by the different emission lifetimes. The fluorescence has a mean emission lifetime of about 3.6 ns whereas the mean emission lifetime of the phosphorescence is 231 μs in oxygen free water at ϑ = 20 °C. In Fig. 11 the procedure is shown schematically. The fluorescence is measured at the moment of excitation t_0. After a delay time of 1 μs the measurement of the phosphorescence is started at t_1. The corruption of the fluorescence data by phosphorescence can be neglected, because the phosphorescence intensity is two orders of magnitude smaller than the fluorescence intensity in our measurements.

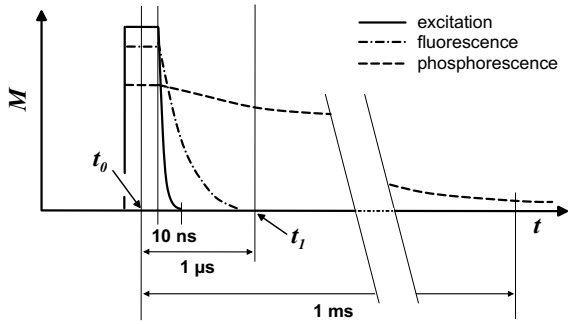

Figure 11: Scheme of the time dependent behavior of excitation and luminescence emission.

The analog signals of the photo-multipliers are converted to digital signals with a fast A/D-conversion card (Spectrum GmbH, Germany) with a frequency of 1 MHz per channel so that the temporal resolution of the intensity measurement is 1 μs. The measuring duration after a single laser shot is about 1 ms. The different jitters of the laser and the measuring card were equalized with an external synchronizing clock and a pulse/delay generator (Quantum Composers Inc., USA). The remaining fluctuations in excitation intensity of the laser dye are measured with an additional photo-multiplier simultaneously and are used to correct the indicator fluorescence emission.

Liquid thickness measurements using a cylinder cuvette filled to different film heights have shown a linear dependence of fluorescence intensity on liquid film thickness in the range of $d_\mathrm{f} = 0.4..2.5$ mm. The distance between the end of the light conductor and the bottom of the petri dish was 4 mm. This is the same distance as in the falling film experiments between the light conductors and the bottom plate of the evaporator. Assuming the same linearity in the falling film experiments the fluorescence measurements are evaluated on the basis of the determined dependance on d_f. According to the thickness measurement at the cylinder cuvette dish the error in film thickness is 2.1% standard deviation in respect to the mean value of 1 mm film thickness.

With the specified measuring device it is possible to simultaneously obtain information about film thickness and temperature distribution every 20 ms. The phosphorescence signal which is used to reconstruct the temperature distribution has a temporal resolution of 1 μs.

4.2 Falling Liquid Film Setup

The experimental setup for the temperature distribution measurement in a falling liquid film is shown schematically in Fig. 12. The main reservoir contains demineralized water degassed with purified nitrogen 5.0. OxiSorb® (Messer-Griesheim GmbH, Germany) is used to remove traces of moisture, oxygen and hydrocarbons from the nitrogen gas supply. The mechanism is a chemisorption of the impurities with reactive chromium compounds. The dissolved oxygen is stripped from the water by nitrogen bubbles. The oxygen concentration is reduced down to 10^{-6} mol/m^3 which is the lower bound of the indicator sensitivity range for measurement of concentration distributions, see Schagen and Modigell (2005) [23]. After degasification the luminescence indicator biacetyl is added in a concentration of 11.4 mol/m^3. In this concentration biacetyl does not change the physical properties of the liquid significantly. A measurement of the surface tension of the aqueous biacetyl solution with a du Nuoy tensiometer results in a value of 72.5×10^{-3} N/m. The surface tension of pure water is 72.75×10^{-3} N/m at 20 °C.

The conditioned liquid flows out of the main reservoir into the film device, which can be inclined relative to the horizontal plane in the range of φ = 0 to 60°. The liquid flows out of a storage chamber through a manually adjustable slit into the heating chamber with an overall length of L = 630 mm, a width of W = 70 mm and a height of H = 30 mm. With separate gas streams the storage and the main chamber are rinsed to form a nitrogen atmosphere above the liquid surfaces to prevent additional quenching of the phosphorescence by molecular oxygen. A magnetic

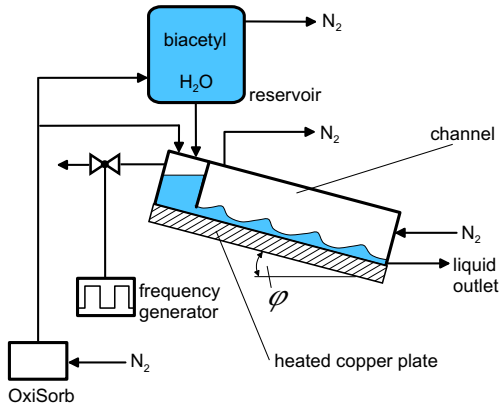

Figure 12: Scheme of the experimental setup.

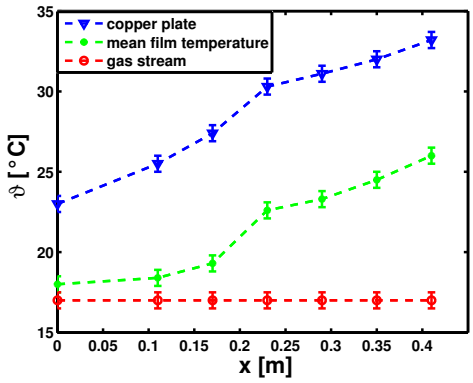

Figure 13: Surface temperature of the copper plate, mean film temperature and gas stream temperature during the experiment.

valve with an adjustable control frequency is installed at the outlet of the storage chamber stream to excite the liquid in this chamber with pressure pulses. Thus the liquid forms a developing laminar-wavy flow in the evaporator.

The falling liquid film is heated from below using an electrically heated copper plate of 6 mm height, 630 mm length and 130 mm width. The copper plate can be heated up to a maximum temperature of $\vartheta_{\mathrm{w,max}}$ = 60 °C if no liquid film flows down the plate. During the experiment the temperature of the copper plate increases from 23 °C at the liquid inlet to 33.2 °C at the position x = 410 mm as can be seen in Fig.13. These measurements are used as an initial guess for the wall temperature in the evaluation procedure. An integral temperature of the liquid film was invasively measured with a thermocouple. The physical properties of the liquid are calculated with these temperatures and are assumed to be constant while evaluating the phosphorescence signals. For the evaluation point at x = 230 mm the temperature is ϑ = 22.6 °C. The properties of water at this temperature are ρ = 997.64 kg/m^3, c_p = 4.181 kJ/(kg K), λ = 0.598 W/(m K), $\eta = 0.949\times10^{-3}$ kg/(m s) and the Prandtl number is 6.66. For the evaluation point at x = 350 mm the temperature is ϑ = 24.7 °C. The properties of water at this temperature are ρ = 996.68 kg/m^3, c_p = 4.182 kJ/(kg K), λ = 0.605 W/(m K), $\eta = 0.915\times10^{-3}$ kg/(m s) and the Prandtl number is 6.36. The values are taken from the CRC Handbook of Chemistry and Physics [12] and were kept constant in the evaluation procedure at each measuring point. The temperature of the counter-current gas stream remained constant at 17 °C. All temperatures were measured with an accuracy of ± 0.5 °C (Ahlborn Therm 2250-1).

5 Experimental Data and Evaluation

The settings used during the experiments on the laminar-wavy liquid film flowing down the inclined and heated plane are summarized in table 1.

Table 1: Parameters of the experimental setup.

Design parameter	name	value
liquid side Reynolds number [-]	Re_l	126
gas side Reynolds number [-]	Re_g	200
inclination angle [°]	φ	2
liquid flow rate [l/h]	$\dot{V}_\mathrm{l}$	32
gas flow rate [l/h]	$\dot{V}_\mathrm{g}$	551
disturbance frequency [Hz]	f_d	2
initial liquid temperature [°C]	ϑ_0	18
constant gas temperature [°C]	ϑ_g	17

5.1 Film Thickness and Wave Velocity

In Fig. 14 the film thickness versus time obtained from fluorescence measurements at position x = 230 mm is depicted. At this position the velocity distribution in flow direction can be approximated with the parabolic profile described by Eq. 6. The mean of fluorescence emission is based on 2000 data points measured in an interval of 40 s. This result constitutes the calibration value that corresponds to the mean film thickness predicted by Nusselt theory [18]

$$d_{\mathrm{f,m}} = \left(\frac{3\,\nu^2\,Re_\mathrm{l}}{g\,\sin\varphi}\right)^{1/3} = 1.04\times10^{-3}\,\mathrm{m}. \qquad (11)$$

Experimental values of Brauer (1961) [8] for vertical films and Al-Sibai (2005) [5] for inclined wavy films confirm the relation of Nusselt for the film thickness.

In Fig. 14 the course of the film thickness over time is depicted relative to the mean film thickness. Looking at the first and the third wave three characteristic regions of a single wave can be identified. The capillary wave region in front of the wave hump, which consists of the wave crest and the wave back, and the substrate behind the wave back. The maximum height of the wave peaks with respect to the mean film thickness is about 55 %. The minimal film

thickness with respect to the mean film thickness of about 40 % is located in front of the wave hump.

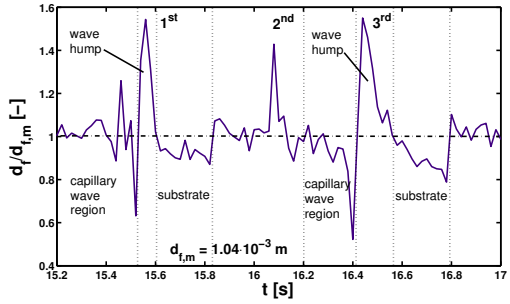

Figure 14: Film contour at measuring point x=230 mm for Re=126.

Analyzing the fluorescence data leads to the mean wave length λ_w = 0.18 m and the mean wave velocity u_w = 0.4 m/s. From a Fourier analysis the primary wave frequency can be determined as f_w = 2 Hz which corresponds to the excitation frequency. Higher order frequencies which can be found in the power spectrum result from the capillary waves in front of the main wave.

The film surface contour at the measuring point is not exactly periodic and equal in shape. One reason is that in the laminar-wavy liquid flow the waves are not fully developed hydrodynamically at the measuring point. This is in accordance with results of Ramaswamy et al. (1996) [19] who showed in direct numerical simulations that with increasing Reynolds number the length of the wave developing region increases too. Already at a Reynolds number of Re_l = 60 and an inclination angle $\varphi = 6.4°$ the wave developing region reaches a length of 0.4 m.

5.2 Temperature Distributions

The temperature distribution is obtained from the decay of phosphorescence intensity. Such a phosphorescence intensity decay curve is measured with a temporal resolution of 1 μs. For the reconstruction of a temperature profile the phosphorescence decay within $\approx$ 0.6 ms is used. The spatial resolution depends on the number of points to which the temperature distribution is numerically mapped in the evaluation procedure. Here spatial resolution is about 30 μm in y-direction.

In this section the results for the temperature distributions for the third wave of Fig. 14 and a wave at the position x=350 mm are presented.

Evaluation of the phosphorescence signals obtained from measurements in these waves lead to the temperature fields shown in Figs. 15 and 16. It can be seen that the surface temperature as well as the temperature gradients in y-direction differ along the wave. In the wave crest and the wave back the temperature gradient is steeper than in the capillary wave region. The maximum change in the gradient along the wave can be localized in front of the wave peak. The wave hump, in which a large amount of mass with lower temperature is transported, flattens the temperature boundary layer of the substrate, as shown in Fig. 15. The surface temperature in the wave crest and the wave back varies from 21.7 to 23 °C in this wave. In the capillary wave region a nearly constant temperature of 24 °C is reached. In the wave at position x=350 mm the colder region is concentrated in the wave hump which is in congruence with numerical simulations of several authors ([1, 16]) for developing solitary waves.

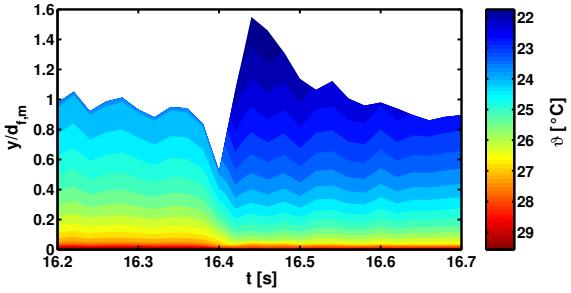

Figure 15: Iso temperature lines along the wave at position x=230 mm for Re=126.

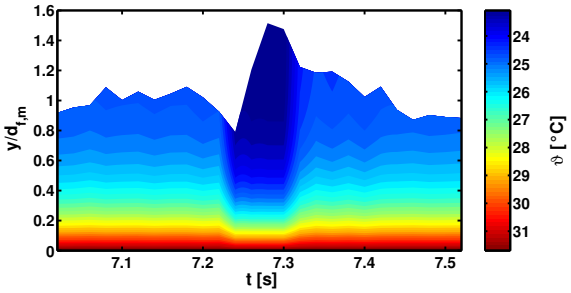

Figure 16: Iso temperature lines along the wave at position x=350 mm for Re=126.

5.3 Local Instantaneous Heat Transfer Coefficient

In investigations on heat transfer in falling liquid film evaporators or reactors often a constant local heat transfer coefficient is assumed. As a result of the proposed measurement method it can be shown that this assumption is a simplification especially in the case of a wavy film.

The local heat transfer coefficient for the considered case is defined as

$$\alpha_w = -\frac{\lambda}{\Delta\vartheta_w}\left.\frac{\partial\vartheta}{\partial y}\right|_{y=0} \qquad (12)$$

with the index w denoting the wall. Heat transfer is driven by the overall temperature difference, which is in the case of transfer from the wall to the liquid is defined as $\Delta\vartheta_w = \vartheta_w - \vartheta_i$. In Figs. 17 and 18 the courses of the local heat transfer coefficient normalized to the respective mean values are depicted.

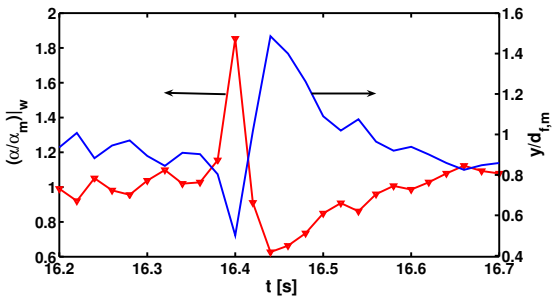

Figure 17: Local heat transfer coefficient along the wave at position x=230 mm.

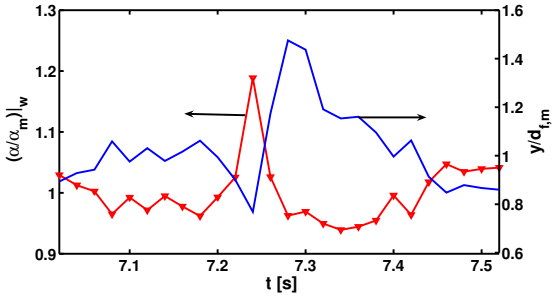

Figure 18: Local heat transfer coefficient along the wave at position x=350 mm.

The mean transfer coefficient at the heated wall is determined as $\alpha_{\mathrm{w,m}}$ = 2190.5 W/(m^2 K) for the wave at x=230 mm and $\alpha_{\mathrm{w,m}}$ = 1857 W/(m^2 K) for the wave at x=350 mm. The decrease of the second mean value is caused by less steep temperature gradients from the wall into the liquid and a slight increase in the driving temperature difference. Both curves of the local heat transfer coefficient show a significantly higher value in front of the wave and a minimum beneath the wave hump. After that the curves increase slowly to their mean values. Numerical simulations of Adomeit et al. [1] for a Reynolds number of 50 and a Prandtl number of 1 are in good agreement with our experimental results, see Fig. 19. The course of the dimensionless local heat transfer coefficient is qualitatively the same. Especially the peak in front of the wave and the behavior beneath the wave is congruent.

6 Conclusion

A new measurement method for the determination of the temperature distribution with high spatial and temporal resolution in thin liquid films is presented. This method is based on the temperature dependent emission lifetime of an optical indicator. First results for the heat transport in a wavy falling liquid film flowing down a heated plane are presented exemplarily.

With the temperature profiles determined from measurements in a laminar-wavy falling liquid film the local heat transfer coefficients are calculated. The calculations

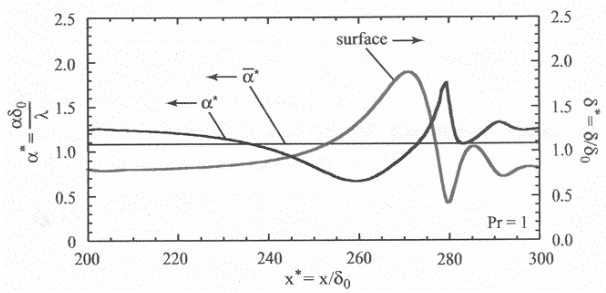

Figure 19: Wave surface and instantaneous dimensionless local heat transfer coefficient α^* at Re=50, taken from Adomeit et al. [1].

show that the local heat transfer coefficient is not constant along the wave as it is often assumed. Here the maximum value is reached in front of the wave between the capillary wave region and the wave crest. The results also indicate a wave induced intensification of heat transfer due to convective transport perpendicular to the wall in the central region of the film.

Further investigations of the kinetic phenomena covering single waves will be done for laminar-wavy falling liquid films flowing down a heated plane at different positions in flow direction varying Reynolds number and inclination angle of the evaporator. The results will be the basis for research of coupled heat and mass transfer mechanisms including chemical reactions in falling liquid films.

Acknowledgement – The authors gratefully acknowledge the financial support of the Deutsche Forschungsgemeinschaft (DFG) within the Collaborative Research Center (SFB) 540 "Model-based Experimental Analysis of Kinetic Phenomena in Fluid Multi-phase Reactive Systems".

References

[1] P. Adomeit, A. Leefken, U. Renz, Experimental and numerical investigations on wavy films, Proceedings of the 3rd European Thermal Science Conference, 2 (2000) 1003-1009.

[2] K. Alhusseini, M. Tuzla, J.C. Chen, Falling film evaporation of single component liquids, Int. J. of Heat and Mass Transfer, 41 (1998) 1623-1632.

[3] S.V. Alekseenko, V.E. Nakoryakov, P.G. Pokusaev, Wave flow of liquid films, Begell House, New York, 1994.

[4] M. Almgren, The natrual phosphorescence lifetime of biacetyl and benzil in fluid solution, Photochemistry and Photobiology, 6 (1968) 829-840.

[5] F. Al-Sibai, *Local and instantaneous distribution of heat transfer rates and velocities in thin wavy films*, PhD thesis, RWTH Aachen, Aachen, 2005.

[6] F. Al-Sibai, A. Leefken, U. Renz, Local and instantaneous distribution of heat transfer rates and velocities in thin wavy films, Proc. of Eurotherm 71 on Visualization, Imaging and Data Analysis in Convective Heat and Mass Transfer, Reims, France, October 2002, pp. 28-30.

[7] F. Al-Sibai, A. Leefken, U. Renz, Local and instantaneous distribution of heat transfer rates through wavy films, Int. J. of Thermal Science, 41 (7) (2002) 658-663.

[8] H. Brauer, Grundlagen der Einphasen- und Mehrphasenströmungen, Verlag Sauerländer, Aarau und Frankfurt am Main, pp. 673, 1961.

[9] N. Brauner, D.M. Maron, Characteristics of inclined thin films, waviness and the associated mass transfer, Int. J. Heat and Mass Transfer, 25 (1) (1982) 99-110.

[10] H.L.J. Bäckström, K. Sandros, The quenching of the long-lived fluorescence of biacetyl in solutions, Acta Chemica Scandinavica, 12 (1958) 823-832.

[11] A.T. Conlisk, Analytical solutions for the heat and mass transfer in a falling film absorber, Chem. Eng. Science, 50 (4) (1995) 651-660.

[12] D.R. Lide (Editor-in-Chief), CRC Handbook of Chemistry and Physics, CRC Press LLC, Boca Reaton, 80^{th} Edition, 2000.

[13] K. Hishida, J. Sakakibara, Combined planar laser-induced fluorescence-particle image velocimetry technique for velocity and temperature fields, Exp. in Fluids, 29 (2000) 129-141.

[14] J.D. Killion, S. Garimella, A critical review of models of coupled heat and mass transfer in falling-film absorption, Int. J. of Refrigeration, 24 (2001) 755-797.

[15] V.V. Lel, A. Leefken, F. Al-Sibai, U. Renz, Extension of the Chromatic Confocal Imaging Method for Local Thickness Measurements of Wavy Films, Proceedings of 5^{th} Int. Conf. on Multiphase Flow, ICMF'04, Yokohama, Japan, May 30 - June 4 2004, 20 Paper No. 155.

[16] A. Miyara, Numerical analysis on flow dynamics and heat transfer of falling liquid films with interfacial waves, Heat and Mass Transfer, 35 (1999) 298-306.

[17] S. Miladinova, S. Slavtchev, G. Lebon, J.C. Legros, Long-wave instabilities of non-uniformly heated falling films, J. Fluid Mechanics, 453 (2002) 153-175.

[18] W. Nusselt, Die Oberflächenkondensation des Wasserdampfes, Z. VDI, 60 (1916) 514-546.

[19] B. Ramaswamy, S. Chippada, S.W. Joo, A full-scale numerical study of interfacial instabilities in thin-film flow, J. Fluid Mech., 325 (1996) 163-194.

[20] R.M. Roberts, H.C. Chang, Wave-enhanced interfacial transfer, Chem. Eng. Science, 55 (2000) 1127-1141.

[21] A. Günther, P. Rudolf von Rohr, Influence of the optical configuration on temperature measurements with fluid-dispersed TLCs, Exp. in Fluids, 32 (2002) 533-541.

[22] J. Sakakibara, R.J. Adrian, Whole field measurement of temperature in water using two-color laser induced fluorescence, Exp. in Fluids, 26 (1999) 7-15.

[23] A. Schagen, M. Modigell, Luminescence technique for the measurement of local concentration distribution in thin liquid films, Exp. in Fluids, 38 (2005) 174-184.

[24] F.K. Wasden, A.E. Dukler, A numerical study of mass transfer in free falling films, AIChE J., 36 (1990) 1379-1390.

[25] L. Wolfersdorf, Inverse und schlecht gestellte Probleme - Eine Einführung, Sitzungsberichte der sächsischen Akademie der Wissenschaften zu Leipzig, 124 (5) (1994).